33RD CONGRESS
OF THE INTERNATIONAL COUNCIL
OF THE AERONAUTICAL SCIENCES
STOCKHOLM, SWEDEN, 4-9 SEPTEMBER, 2022

ICAS 2022 SWEDEN

USING ACTIVE FLOW CONTROL TO IMPROVE THE AERODYNAMIC PERFORMANCE OF THE NEXT GENERATION CIVIL TILT ROTOR AIRCRAFT

J.B. Vos[1], A. Gehri[1], H. Truong[2], A. Marouf[2] & Y. Hoarau[2]

[1]CFS Engineering, EPFL Innovation Park, Batiment A, 1015 Lausanne, Switzerland
[2]University of Strasbourg, ICUBE Research Institute, Mechanical Department, Strasbourg, 67500, France

Abstract

This paper presents the results of studies using so called Zero Net Mass Flux (ZNMF) actuators for active flow control on the Next Generation Civil Tilt Rotor Technical Demonstrator (NGCTR-TD) aircraft. The Next Generation Civil Tilt Rotor (NGCTR-TD) is a a novel concept that combines the benefits of a helicopter with the speed and the capabilities of a fixed wing aircraft. The range and speed are comparable to that of a fixed wing aircraft, but the aircraft can land and take-off vertically, and when needed, can hover on a fixed position over ground.
The European Funded CleanSky2 project AFC4TR (Active Flow Control for Tilt Rotor Aircraft) will investigate the use of ZNMF devices to increase the aerodynamic efficiency. In the first phase of the project unsteady CFD simulations were made for the flow over the NGCTR-TD aircraft to identify critical flow regions that could benefit from ZNMF devices. In the second phase of the project unsteady CFD simulations were made for the flow over the NGCTR-TD aircraft using ZNMF devices. In the third phase of the project optimization studies are made to identify the the optimal parameter settings and the best locations of the ZNMF devices.

Keywords: keywords list (Flow Control, CFD, ZNMF devices)

1. Introduction

Although the Covid pandemic has had a large influence on travel by air, it is still expected that passenger and freight traffic will increase continuously over the next two decades. One of the main challenges that the aviation industry is facing today is to reduce its negative impacts on the environment. The Advisory Council for Aviation Research and Innovation in Europe (ACARE) in its 'FlightPath 2050' [1] has set as target a 90% reduction in NOx emissions, 65% reduction in perceived aircraft noise and 75% reduction in fuel burn by 2050 compared to the year 2000.
The Next Generation Civil Tilt Rotor (NGCTR-TD) is a a novel concept that combines the benefits of a helicopter with the speed and the capabilities of a fixed wing aircraft. The range and speed are comparable to that of a fixed wing aircraft, but the aircraft can land and take-off vertically, and when needed can hover on a fixed position over ground. A Technology Demonstrator will be built to validate its architecture, technologies /systems and operational concepts. One of the studies to be made concern the use of Active Flow Control using so called ZNMF (Zero Net Mass Flux) devices to overcome flow separations, which might lead to an increase in aerodynamic efficiency, and a reduction in noise. This might decrease the fuel burn, and the associated NOx and CO2 emissions. Although Active Flow Control has been studied for more than 50 years, it's application is still not seen on aircraft for various reasons among them integration and power supply, reliability and certification requirements. Designing a novel aircraft configuration that from the start envisages the use of ZNMF devices might lead to a breakthrough in the use of these devices for future, and possibly, existing aircraft.
Active Flow Control has been studied for several decades, and a large variety of actuator systems exist that might be classified according input energy (mechanical, fluidic or thermal), orientation relative

to the external flow, frequency response and bandwidth [2]. ZNMF devices belong to the category of fluidic devices, and different studies (both experimental and using CFD) demonstrated that these devices can be used for the control of flow separations. The first ZNMF device was mentioned by Ingard and Labate [3] in 1950, and they used standing waves in an acoustically driven circular tube to induce an oscillating velocity field near an orifice end-plate, and observed the formation of the ZNMF jet from opposing trains of vortex rings on both sides of the orifice.
The ZNMF jet is usually produced by a sinusoidal oscillating membrane or piston to alternating force fluid through an orifice into the external flow field and entrain fluid back. During the blowing stroke, the ejected fluid separates at the sharp edges of the orifice and rolls up to form a vortex pair or ring (2D with slot orifice and 3D with circular orifice, respectively). When the membrane begins its suction stroke, the vortex pair or ring is quite far from the orifice and keeps on propagating away due to its self-induced velocity. Hence, the vortex pair or ring can not be entrained back into the cavity, but it will coalesce to synthesize a jet with momentum transfer to the embedding flow. The ZNMF jet has a unique feature compared to the traditional blowing or suction flow control methods, i.e. the ZNMF jet requires neither external fluid supply nor complex piping. This enables the ZNMF jet actuator to have several distinct advantages such as a reduced size and weight, an improved manufacturability, low cost and increased reliability. This makes it today worldwide a very popular flow control device.
The efficiency of ZNMF actuators depends on several parameters of which the key parameters are the frequency of the jet and the ratio of the actuator exit velocity to the free-stream velocity V_{jet}/U_∞ (or the blowing momentum coefficient $C_\mu = V_{jet}^2 D/\frac{1}{2}\rho U_\infty^2 c$).
From the modeling point of view two different methods have been proposed, a modeling of the jet velocity or of the membrane initiating the movement. Studies found in the literature point in the direction that modeling of the flow in the cavity is important to capture the physics of ZNMF devices correctly.
This paper is organized as follows: Section 2 presents the NSMB CFD solver used in these studies, Section 3 discusses the mesh generation for the NGCTR-TD, and Section 4 presents the results of the identification of critical flow regions on the NGCTR-TD that might benefit from the use of ZNMF devices. Section 5 presents the results of 2D and 3D studies using ZNMF devices to determine the most important parameters of these devices. Section 6 discusses the use of the ZNMF devices on the NGCTR-TD configuration.

2. NSMB CFD solver

The Navier Stokes Multi Block solver NSMB [4, 5] was initially developed in 1992 at the Swiss Federal Institute of Technology (EPFL) in Lausanne, and from 1993 on-wards in the NSMB consortium composed of different universities, research establishments and industries. Today NSMB is developed by IMF-Toulouse (IMF Toulouse, France), ICUBE (Strasbourg, France), University of Munchen (TUM, Germany), University of the Army in Munchen (Germany), the Ariane Group (France), RUAG Aviation and CFS Engineering.
NSMB is a parallelized CFD solver employing the cell-centered finite volume method using multi block structured grids to discretize the Navier-Stokes equations. The patch grid and the Chimera grid approach are available to facilitate the grid generation for complex geometries. In addition, the Chimera method is used for simulations involving moving bodies. Various space discretization schemes are available, among them the 2^{nd} and 4^{th} order central schemes with an artificial dissipation and Roe and AUSM upwind schemes from 1^{st} to 5^{th} order. Time integration can be made using the explicit Runge-Kutta schemes, or the semi-implicit LU-SGS scheme. Various methods are available to accelerate the convergence to steady state, as for example local time stepping, multigrid and full multigrid, and low Mach number preconditioning. The dual time stepping approach is used for unsteady simulations.
In NSMB turbulence is modeled using standard approaches as for example the algebraic Baldwin-Lomax model, the one-equation Spalart model [6] (and several of its variants) and the $k-\omega$ family of models (including the Wilcox and Menter Shear Stress models [9]). Several Hybrid RANS-LES models are available, as for example the Delayed Detached Eddy Simulation (DDES) model, [7]. NSMB includes also several transition models solving transport equations [8].
The Arbitrary Lagrangian Eulerian (ALE) approach is available in NSMB to simulate flows over moving bodies or with moving components (the rotor of the NGCTR-TD).

The ZNMF devices were implemented using a small cavity with a time varying velocity boundary condition (both blowing and suction) on the boundary opposite to the jet in order to simulate the vibration of a membrane or a piezo actuator as in a hardware device. The parameters of the boundary condition permit to vary the amplitude and the frequency of the velocity fluctuations of the jet.

3. Mesh Generation Next Generation Civil Tilt Rotor

The grid for the NGCTR-TD was generated using the ANSYS ICEM CFD mesh generator. Both the patch grid as well as the chimera overlapping technique were employed to simplify the mesh generation. The chimera technique permits to create a multi block structured grid for a single configuration, and obtain other configurations through translations and rotations of partial grid elements, for example flap deflections, nacelle rotation etc, see Fig. 1. The patch grid approach was used to reduce the number of grid cells in the far field region.

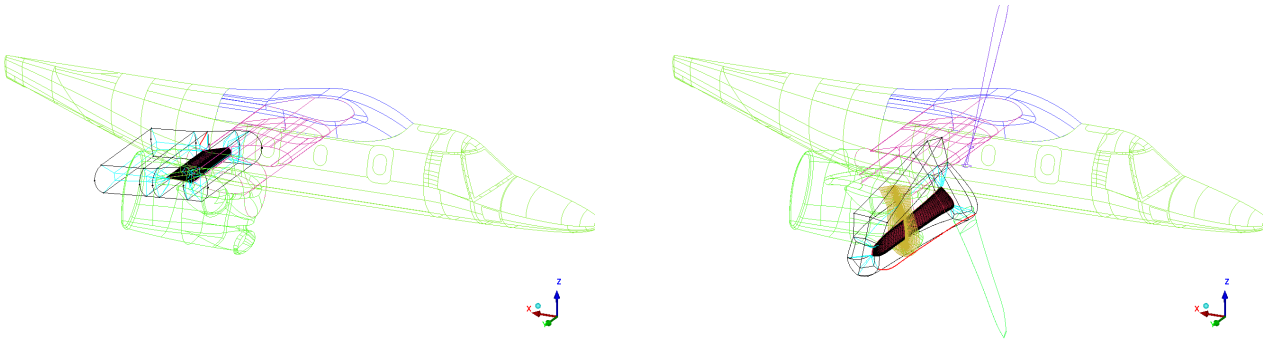

(a) Chimera grid Aileron

(b) Chimera grid rotor blades

Figure 1 – Chimera grids around the aileron and the rotor blades.

O-grid topologies are used to resolve the viscous boundary layers, with a geometric cell distribution normal to solid walls. The first cell height in the normal direction was set to ensure a y^+ value around 1, and the growth ratio of the cells normal to the wall was set to 1.2. The chord-wise spacing was set below 0.1% of the local chord at the leading edge and the trailing edge of the main wing as well as for the blades. The spanwise spacing was set below 0.1% of the semi-span at the root (fuselage junction) and at the tip (nacelle junction). Due to the aileron located close to the nacelle junction, the mesh density at the tip was extended widely in this region. Particular attention was also paid to the refinement of the mesh close to the areas where the ZNMF devices will be placed later in the project.

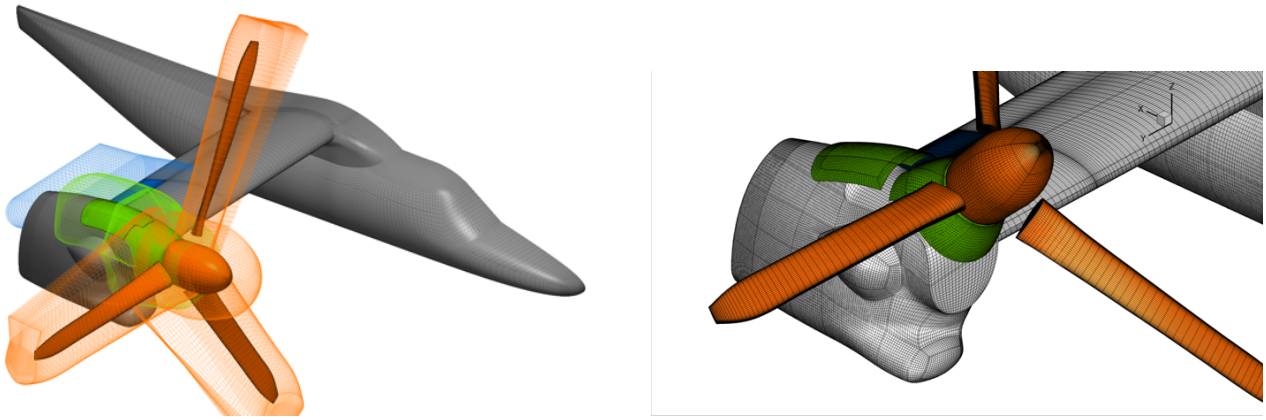

(a) Surface mesh NGCTR-TD

(b) Surface mesh rotated engine and blades

Figure 2 – Surface mesh (left) and volume mesh around chimera components (right).

Once all grid components were generated using ICEM CFD, they are merged together using Python scripts. The NGCTR-TD base line grid had 900 structured blocks, around 14 Million cells, and 7

movable parts. Around 10 Million cells are used for the base grid (fuselage, wing and nacelle, colored in grey in Fig. 2), 600'000 cells for the Aileron (in blue), 800'000 cells for the engine and engine cover (in green), and 2.5 million cells for the blades and hub (in orange).
Thanks to the chimera technique the engine and blades can be easily rotated using a simple Python script. The grid was designed to permit nacelle rotations up to 90^o. Note that when the nacelle is rotated the nacelle cover needs to be moved too.

4. Identification of critical flow regions on the NGCTR-TD that might benefit from ZNMF devices

Unsteady simulations were made for different configurations of the NGCTR-TD, using different simulation conditions (with and without rotor, with and without nacelle deflection and with and without aileron deflection). These calculations were made using the dual-time stepping approach [10] using a fixed outer-time step. The central scheme with artificial dissipation was used for the discretization in space, and the LU-SGS scheme [11] for the integration in pseudo-time (inner loop). Preconditioning was used to accelerate the convergence of the inner loop. The influence of the turbulence model, the grid, the outer time step, the number of inner loop steps and critical constants of the turbulence model parameters on the results were investigated, and permitted to define the strategy to be used for the calculations to identify the critical flow regions. The conclusion of these studies was that an outer timestep of 10^{-4} seconds was sufficient, and that it was important to set the ratio turbulent to laminar viscosity to a value of at least 10'000. The $k-\omega$ SST model [9] gave the best results, in particular for the prediction of flow separations in the junction regions (fuselage-wing and wing-nacelle).
From the large number of simulations made the following three configurations were identified that could benefit from ZNMF devices near stall conditions:

- Case 1: closed gap, nacelle 0^o, aileron deflection 0^o
- Case 2: closed gap, nacelle 50^o, aileron deflection 0^o
- Case 3: opened gap, nacelle 0^o, aileron deflection 35^o downwards

Case 1, see Fig. 3, is concerned with the flow separations near the wing-fuselage and wing-nacelle junctions. Note that due to the movement of the rotor the flow separations are unsteady.

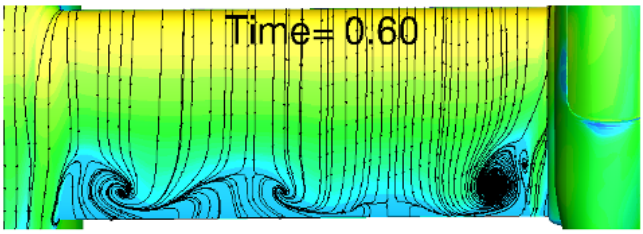

Figure 3 – Skin friction lines on the wing for Case 1.

Case 2, see Fig. 4, is concerned with the case of the rotated nacelle. Due to the tilted nacelle the rotor blades rotate above the wing, as is clearly visible in Fig. 4a.

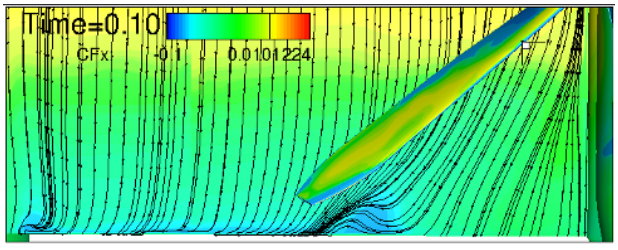

(a) Time = 0.1 seconds

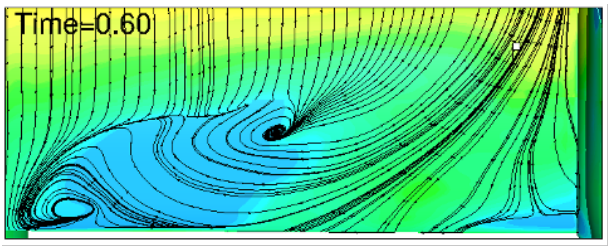

(b) Time = 0.6 seconds

Figure 4 – Skin friction lines on the wing at two time instances for Case 2.

Case 3, see Fig. 5, is concerned with the case of the downwards deflected aileron.

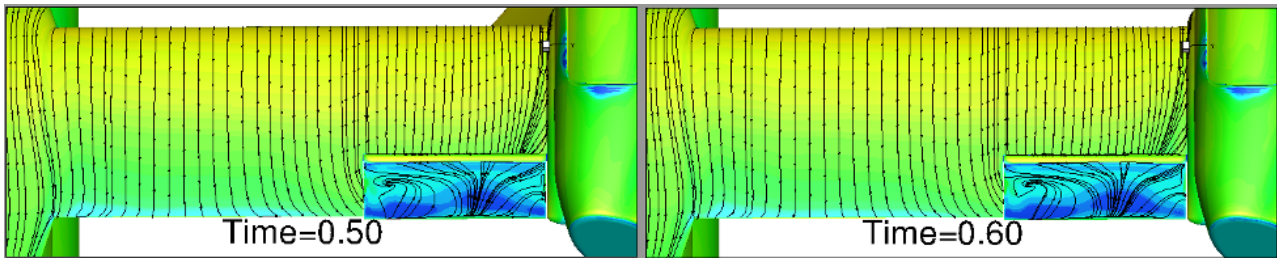

Figure 5 – Skin friction lines on the wing and deflected aileron at two time instances for Case 3.

5. Results of 2D and 3D simulations of flows over airfoils and wings using ZNMF devices

Since unsteady calculations on the NGCTR-TD aircraft are costly, it was decided to make first CFD simulations using ZNMF devices on simple 2D and 3D configurations to determine the most important parameters that affect the use of these devices for flow control. The ZNMF device used in this study is the ASPIC synthetic jet actuator developed by Cedrat technologies in collaboration with ONERA in France [12]. The main advantages of the ASPIC actuator are the high jet velocities and the high activation frequency bandwidth. Figure 6 shows the velocity contours in the flap region without (left) and with (right) activated ZNMF device. As can be seen the ZNMF is able to reduce considerably the flow separation.

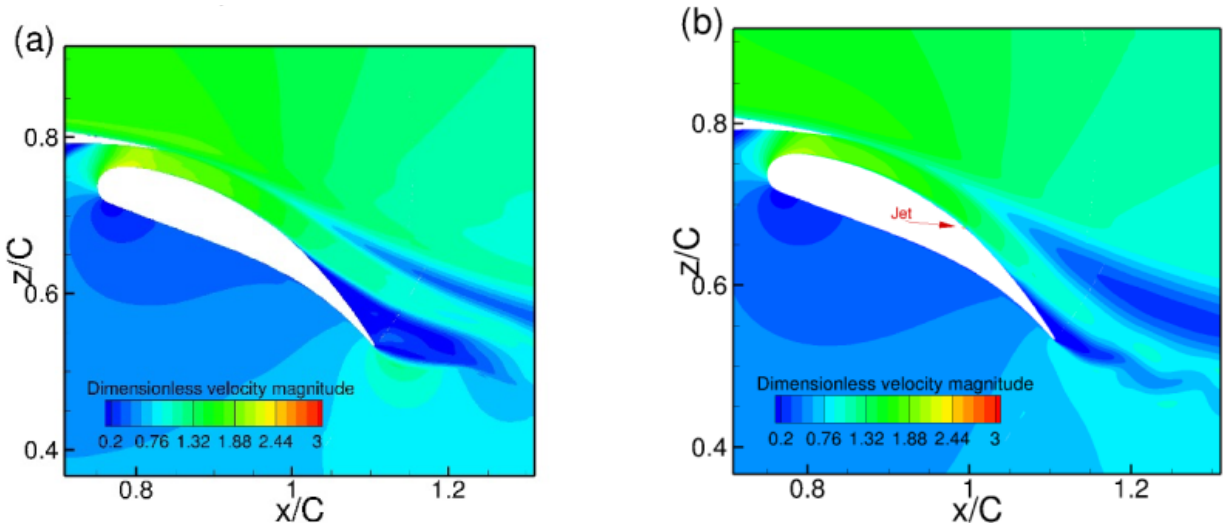

(a) No ZNMF device

(b) ZNMF device with f_a 200 Hz

Figure 6 – Use of ZNMF device for a 2D airfoil with flap.

A large number of parameter studies were made, which showed that

- the influence of the jet on the aerodynamic forces becomes independent of the jet actuation frequency for actuation frequencies above 100 Hz;
- for the different jet velocities studied, it was shown that the highest jet velocity gave the largest increase in aerodynamic performance;
- the location of the ZNMF device should be just upstream of the flow separation;
- in terms of increased aerodynamic efficiency the best results were obtained with a jet angle of 45^o.

A limited number of 3D simulations for the flow over a wing with flap were made to study the 3D influence when using ZNMF devices. In these simulations a flap with a span of $1\ m.$ was equipped with 4 ZNMF devices (each having a width of $150\ mm$). Figure 7 shows the skin friction lines on the

flap for different jet velocities. It can be clearly seen that ZNMF devices are able to delay the flow separation, and that the highest jet velocity has the largest influence. It was also confirmed (but not shown here) that the ZNMF devices should be located just upstream of the flow separation.

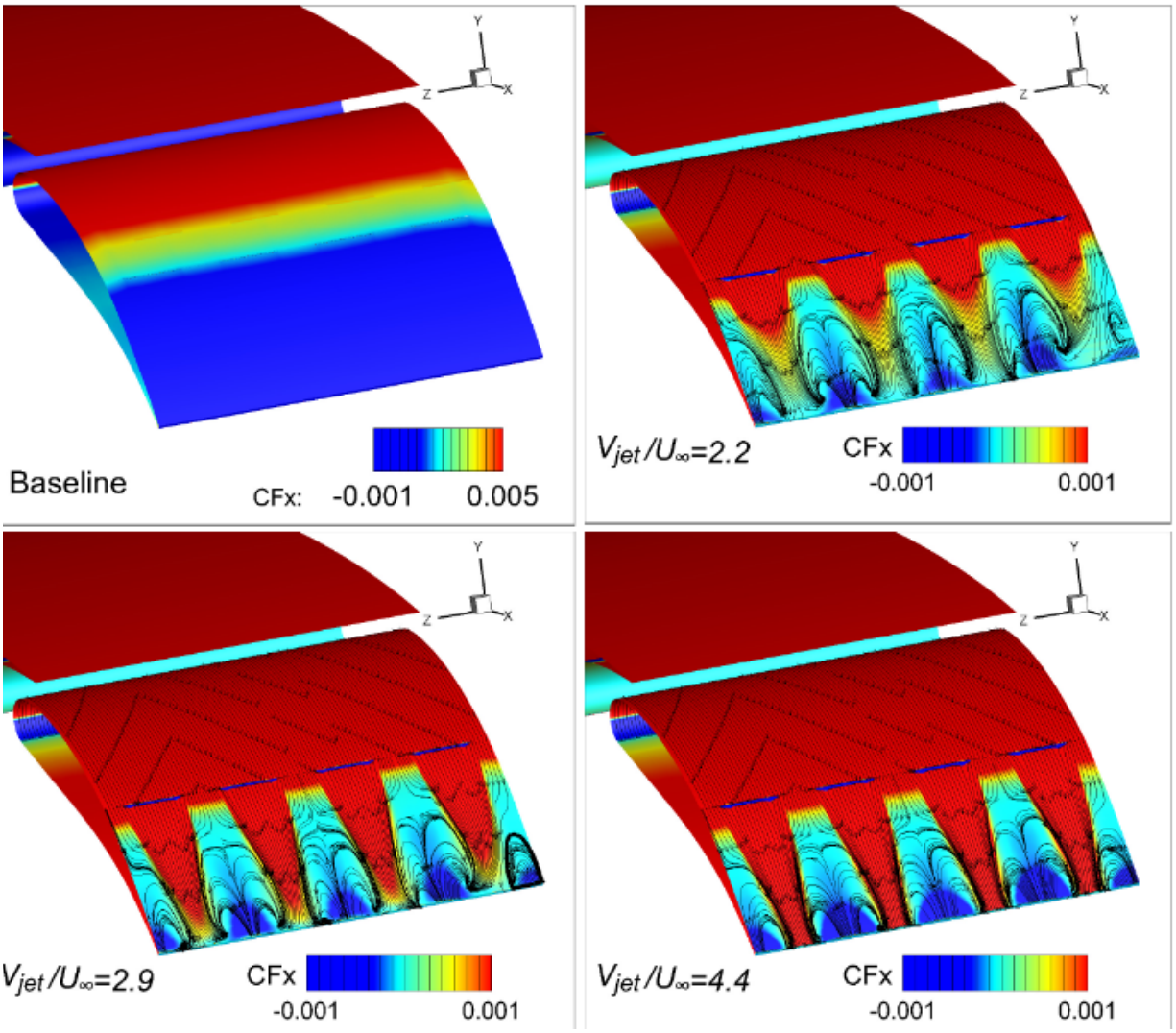

Figure 7 – Skin friction lines on a 3D flap. Different jet velocities are used for the calculations with ZNMF devices.

6. Results of simulations of the NGCTR-TD aircraft using ZNMF devices

The grids for the NGCTR-TD were adapted to include ZNMF devices at different locations, and Fig. 8 shows as example the grid for case 3 (deflected aileron), with several ZNMF devices located on the aileron as illustrated by the refined grid in these regions. A more schematic view used for the optimization studies is given in Fig. 9 for the cases 1 and 3. In this figure different locations of the ZNMF devices are indicated, with location 3 the base position. For case 1 locations 1 and 5 are shifted $\pm 6.4\%$ in the chord direction and locations 2 and 4 $\pm 3.2\%$. For case 3 locations 1 and 5 are shifted $\pm 20\%$ of the aileron chord, and locations 2 and 4 $\pm 10\%$.

6.1 Results case 1.

The unsteady simulations on the NGCTR-TD are costly, also due to the fact that several rotations of the propellor need to be simulated in order to get the flow established. Initial calculations were made with a jet actuation frequency of $65Hz$, which is slightly lower than the recommended actuation frequency of $100Hz$ found in the 2D studies, but permits to make larger time steps.
Figure 10 shows snapshots at $t = 0.26\ secs$ and at $t = 0.46\ secs$ of the x-component of the skin friction

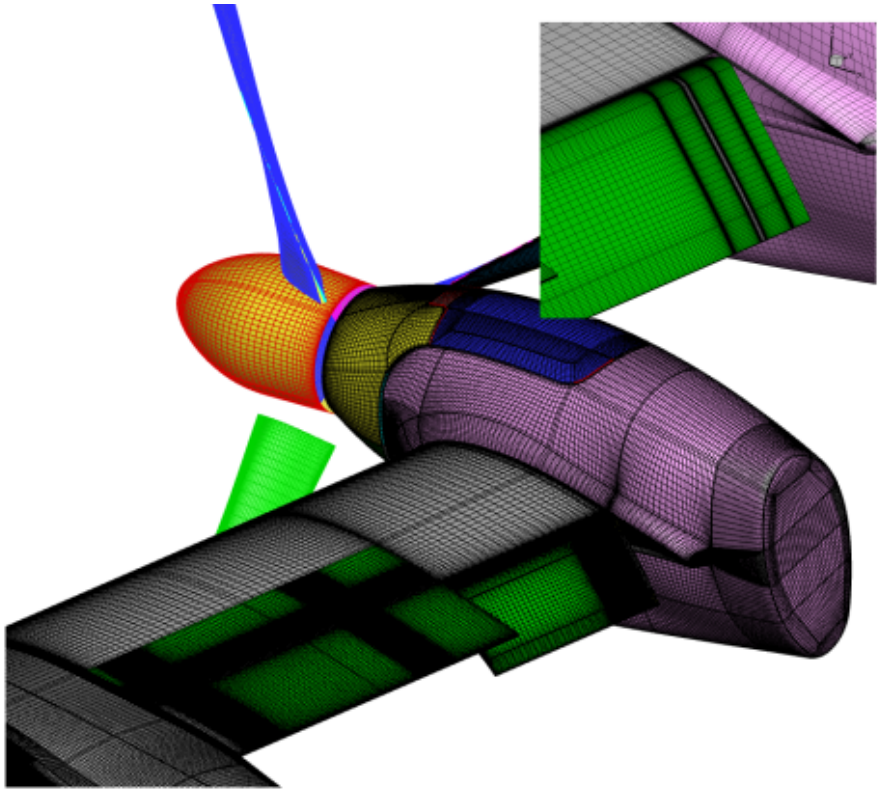

Figure 8 – Grid NGCTR-TD case 3 with ZNMF devices on the aileron.

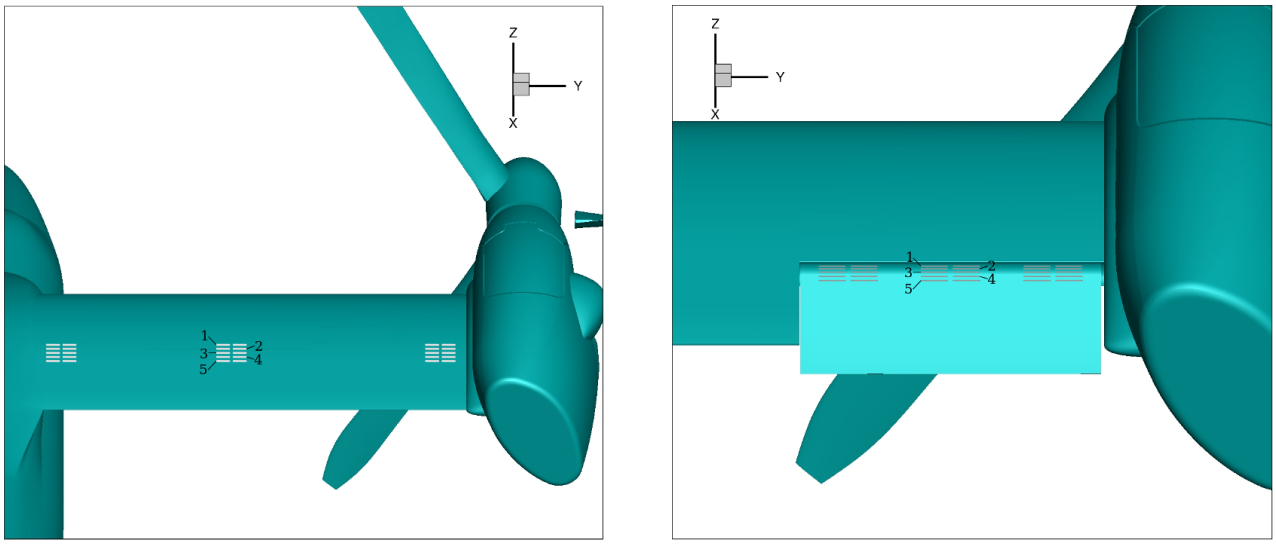

(a) Configuration 1

(b) Configuration 3

Figure 9 – Locations of ZNMF devices on the NGCTR-TD for cases 1 and 3 used in the optimization studies.

vector on the wing, with blue regions indicating separated flow regions. The locations of the ZNMF devices can be recognised by the small regions of high values of the skin friction vector. When using no active flow control (No AFC), one can observe clearly a flow separation near the wing-fuselage at $t = 0.26\ secs$, and at $t = 0.46\ secs$ this flow separation is visible on a substantial part of the wing, but it is less pronounced near the wing-fuselage junction. Activating the ZNMF devices shows that it is possible to reduce the size of the flow separations, but one also observes that flow separations are moving along the wing. The optimal location of the ZNMF device is difficult to determine from these 2 figures, because it depends on the time instance.

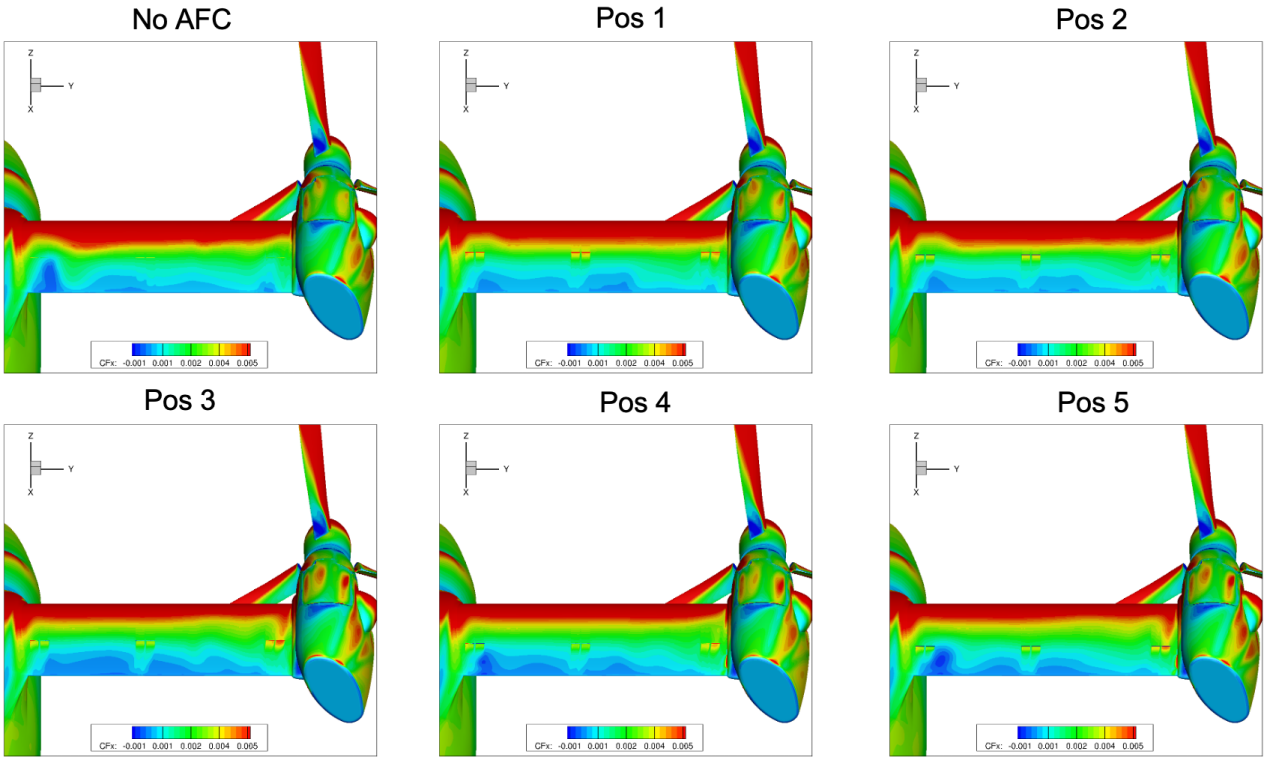

(a) $t = 0.26\ secs$

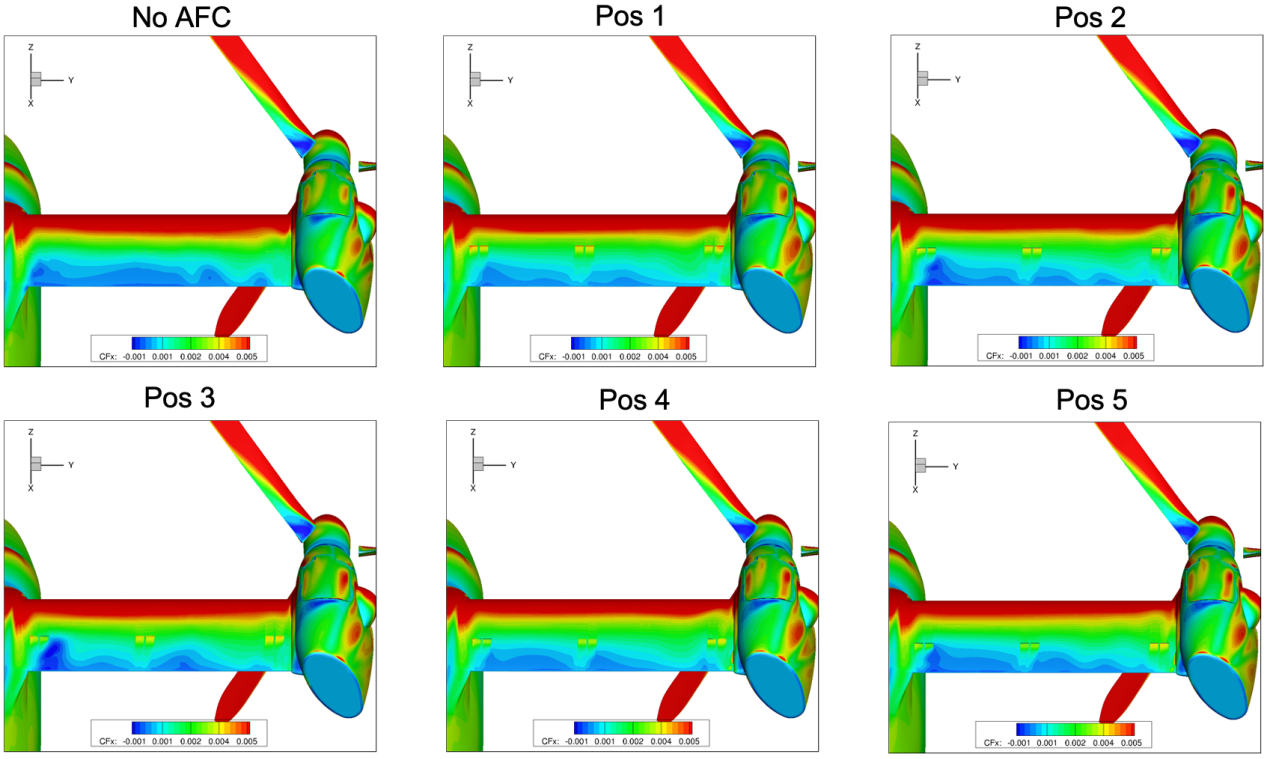

(b) $t = 0.46\ secs$

Figure 10 – Instantaneous skin friction coefficient (C_{f_x}) on the wing for the NGCTR-TD case 1 using different locations of the ZNMF devices.

Fig. 11 shows instantaneous snapshots at $t = 0.26\ secs$ and at $t = 0.46\ secs$ of the skin friction lines near the wing-nacelle junction for case 1, using different locations of the ZNMF devices as well as for the case without ZNMF devices (no AFC). In the simulation without ZNMF devices one clearly sees a small separation bubble near the wing-nacelle junction. Activating the ZNMF devices reduces this separation, but one also observes that the flow separation on the wing increases in size depending on the position of the ZNMF devices. In particular for ZNMF position 3 at $t = 0.26\ secs$ there is a larger flow separation visible on the wing, but at $t = 0.46\ secs$ this flow separation is much smaller, in particular compared to the results without AFC and with the ZNMF devices at positions 2 and 5.
Figure 12 shows the difference with respect to the baseline configuration of the computed CD and CL on the wing. Due to the rotation of the propellor the flow is unsteady, which is clearly visible in the different curves. Figure 13 shows the results of an FFT analysis of the CZ. The frequency of each blade passage is around 24 Hz and one can find this frequency when looking at the different peaks. But other frequencies are also present, and they are affected by the use and location of the ZNMF devices. One can observe dominant frequencies around 48 Hz for the ZNMF devices at P4 and P5, 55 Hz at P1 and P2, and 62 Hz at P3. Further analysis is needed to better understand this behaviour. This shift in dominant frequencies might also be due to the fact that the ZNMF devices are aligned in flow direction (see Fig. 9a), while Fig. 10 shows that the start of the flow separation strongly depends on the location. In particular near the fuselage-wing junction, the flow separation starts much further upstream than at other locations.
The unsteady forces on the wing were for each calculation averaged over several cycles, and Table 1 shows the increase or decrease of the aerodynamic coefficients with respect to the baseline configuration (the configuration without ZNMF devices). As can be seen only position P3 shows a reduction in drag, with at the same time an increase in lift and aerodynamic efficiency. For these simulations the ZNMF devices were aligned, which is not necessarily the optimal strategy because the start of the flow separations on the wing, and near the wing-fuselage and wing-nacelle junctions is not at the same down stream location.

Configuration	ΔCD	ΔCL	$\Delta(CL/CD)$
ZNMF P1	0.00074	0.00126	-0.17255
ZNMF P2	0.00176	-0.00126	-0.45869
ZNMF P3	-0.00123	0.00425	0.37891
ZNMF P4	0.00375	-0.00947	-1.03458
ZNMF P5	0.00363	-0.02000	-1.13347

Table 1 – Difference in CD, CL and Aerodynamic efficiency on the wing with respect to the baseline configuration, NGCTR-TD case 1.

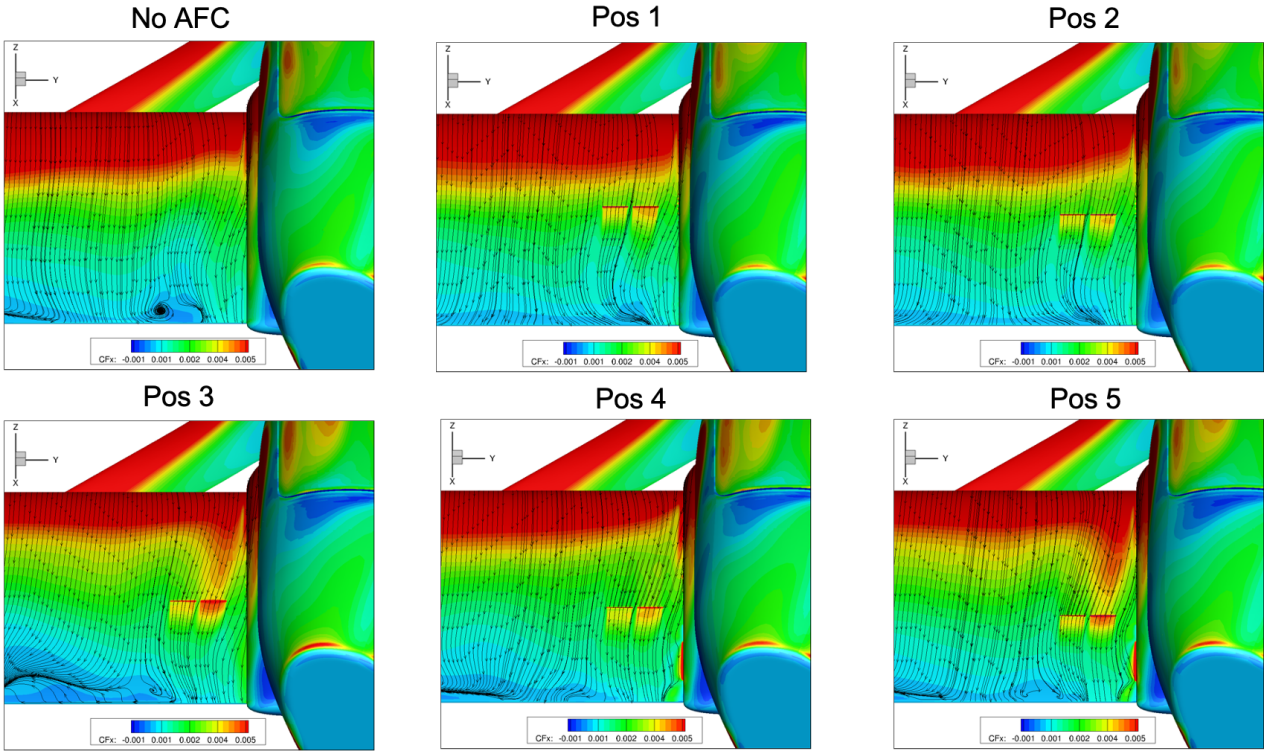

(a) $t = 0.26\ secs$

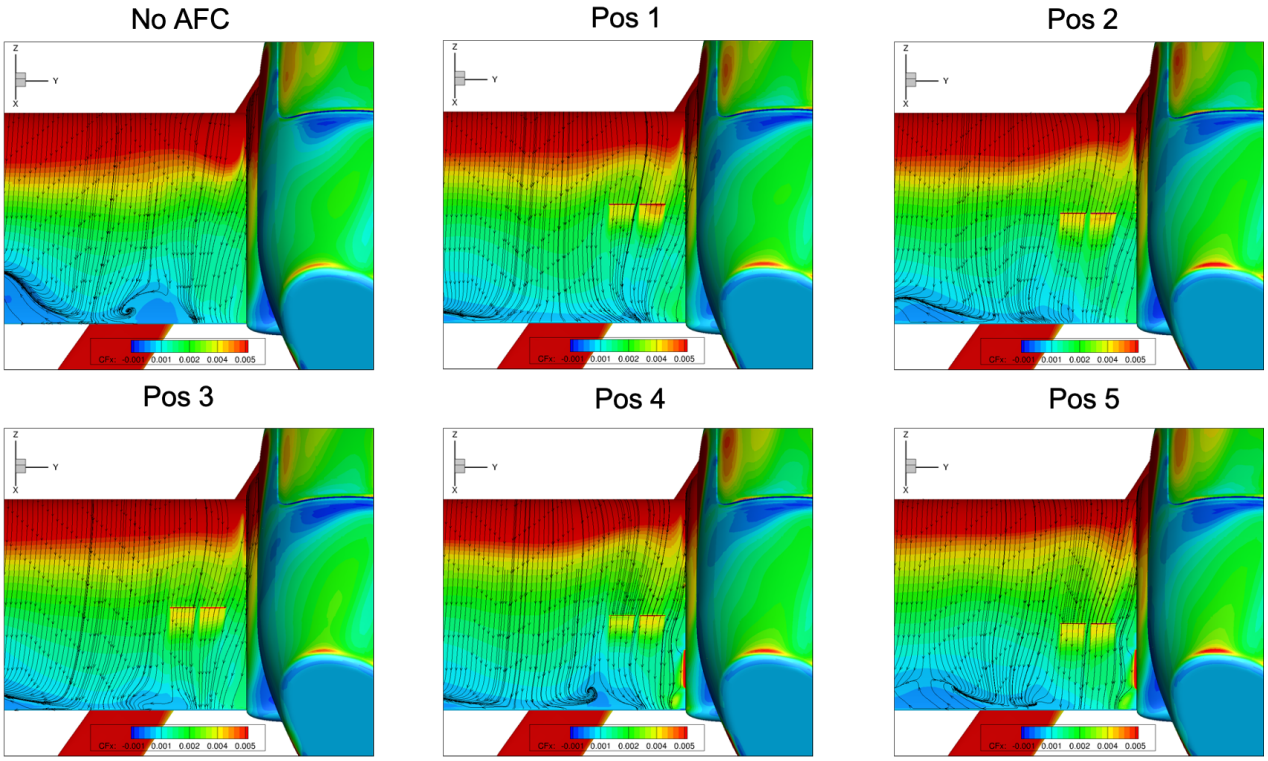

(b) $t = 0.46\ secs$

Figure 11 – Instantaneous skin friction lines near the wing-nacelle junction for the NGCTR-TD case 1 using different locations of the ZNMF devices.

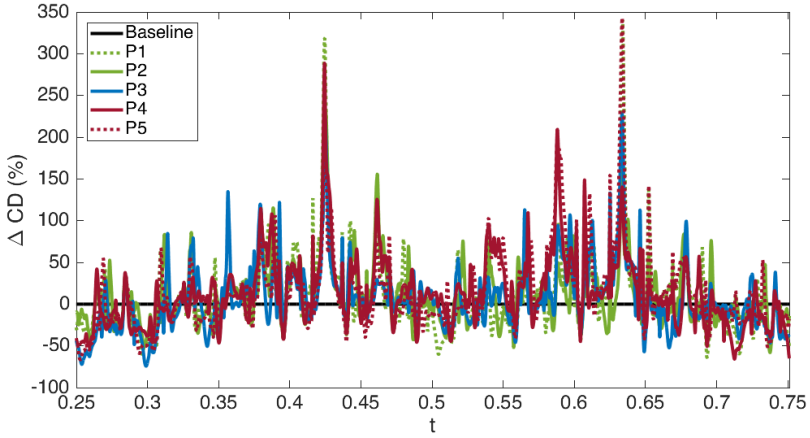

(a) ΔCD

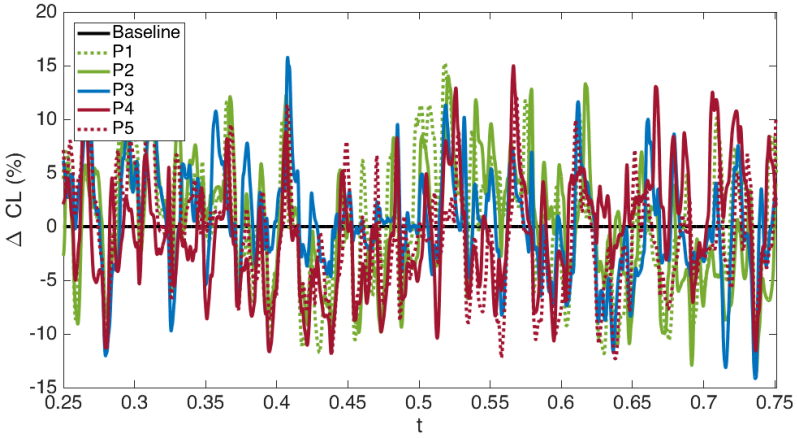

(b) ΔCL

Figure 12 – Instantaneous ΔCD and ΔCL with respect to the base line configuration on the wing of the NGCTR-TD for different positions of the ZNMF devices, case 1.

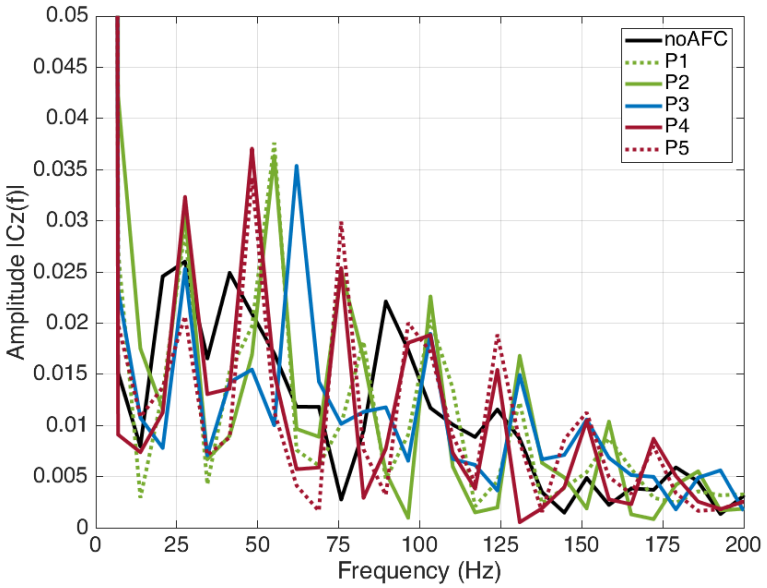

Figure 13 – FFT analysis of the CZ on the wing for case 1.

6.2 Results case 3.

Case 3 is concerned with the NGCTR -TD having a 35^o deflected aileron, with a small gap between the wing and aileron. Figure 14 shows the x-component of the skin friction vector at $t = 0.33\ secs$ and $t = 0.51\ secs$ for different positions of the ZNMF devices, and one can clearly observe the locations of the ZNMF devices. Some delay in flow separation can be observed, in particular at $t = 33\ secs$ for the ZNMF in position P3.

Figure 15 shows the instantaneous ΔCD and ΔCL on the aileron only, and Fig. 16 the FFT analysis of the CZ on the aileron. One clearly observes shifts in the ΔCD and ΔCL as function of the position of the ZNMF device, similar to the results found on the wing. When using No AFC one finds dominant frequencies at 41, 83 and 125 Hz, with ZNMF in positions P2 and P3 one finds dominant frequencies at 50 and 100 Hz, and with the ZNMF in position p4 these frequencies are 60 and 116 Hz.

The unsteady forces on the aileron were for each calculation averaged over several cycles, and Table 2 shows the increase or decrease of the aerodynamic coefficients with respect to the baseline configuration. From this Table one case see that placing the ZNMF device in position 1 reduces the drag, and increases both the lift and aerodynamic efficiency. A higher increase in lift is obtained for the ZNMF device in position 2, but at the expense of a slight increase in drag, and as a result the aerodynamic efficiency is lower compared to the case with the ZNMF in position 1.

Configuration	ΔCD	ΔCL	$\Delta(CL/CD)$
ZNMF P1	-0.00878	0.06198	0.21556
ZNMF P2	0.00497	0.07962	0.19701
ZNMF P3	0.00644	0.07514	0.17770
ZNMF P4	-0.00103	0.05874	0.16818
ZNMF P5	-0.00874	0.03626	0.14210

Table 2 – Difference in aerodynamic forces on the aileron with respect to the baseline configuration, NGCTR-TD case 3.

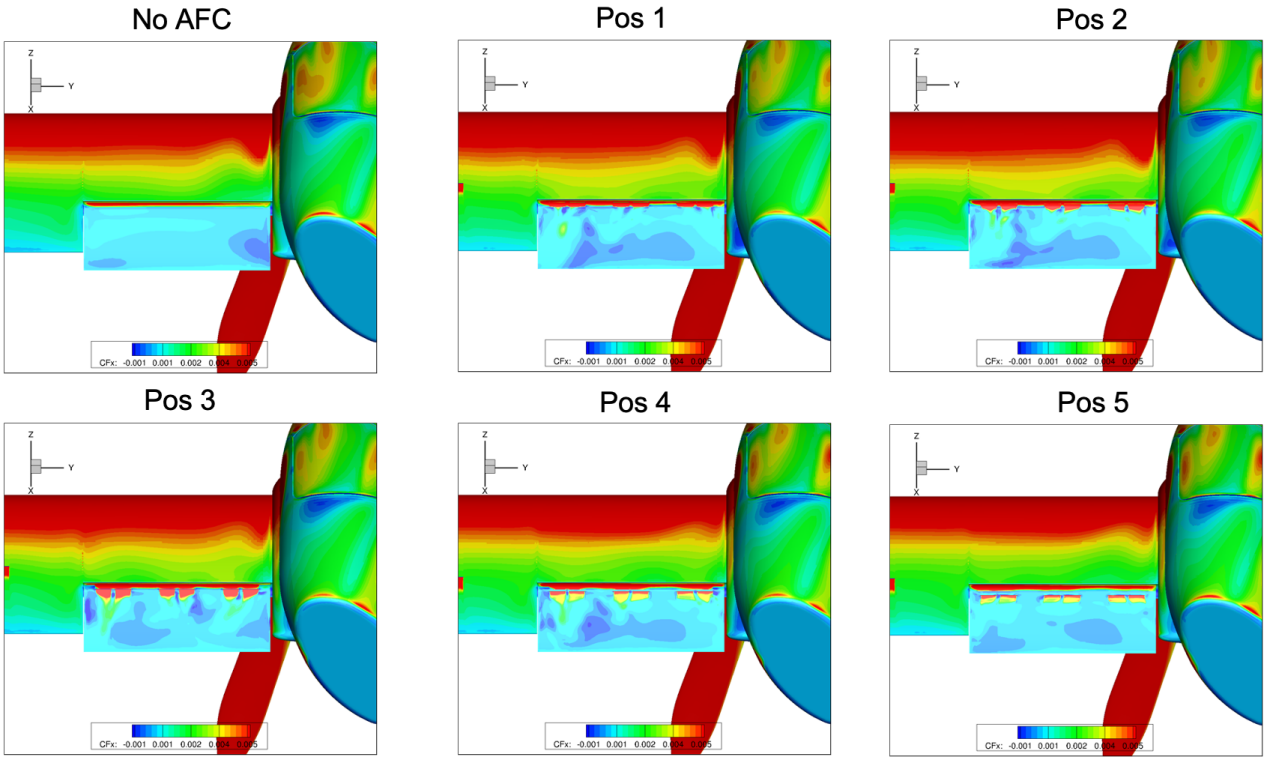

(a) $t = 0.33\ secs$

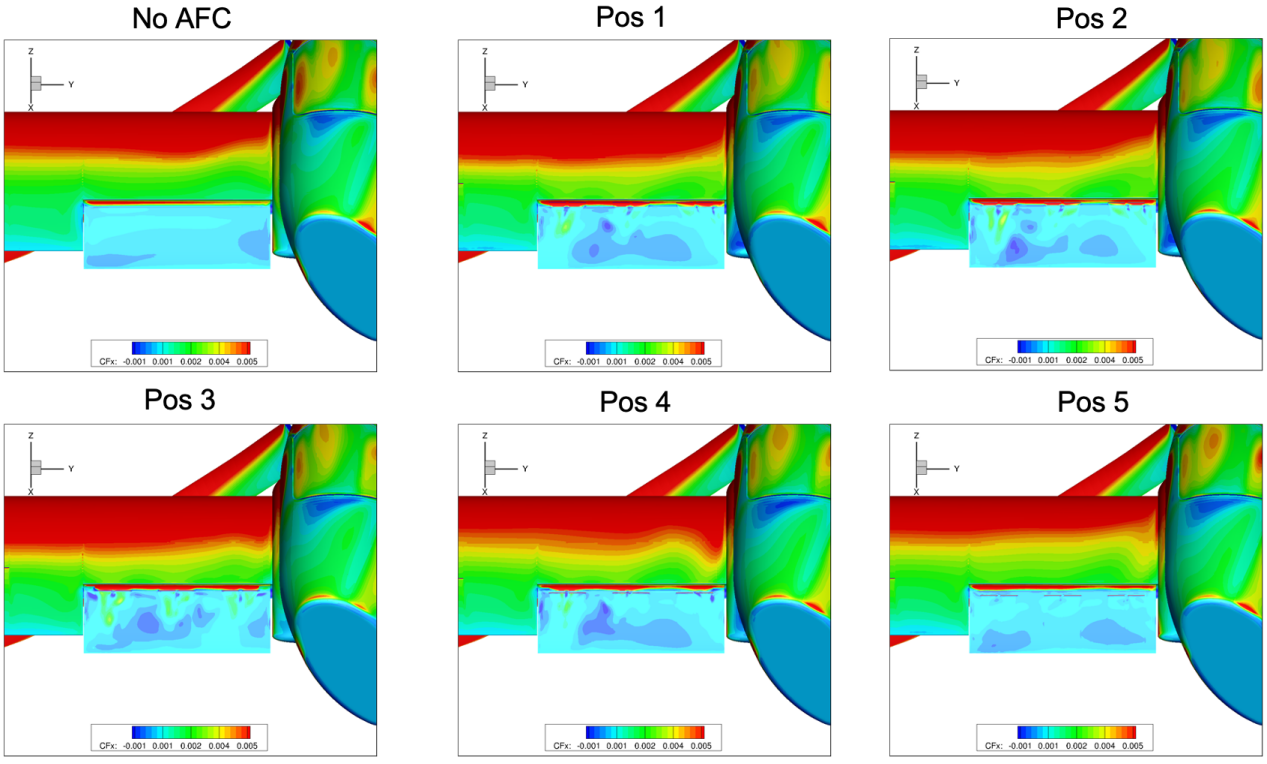

(b) $t = 0.51\ secs$

Figure 14 – Skin friction coefficient (C_{f_x}) on the aileron for the NGCTR-TD case 3 at $t = 0.33\ secs$ and $t = 0.51\ secs$, using different locations of the ZNMF devices.

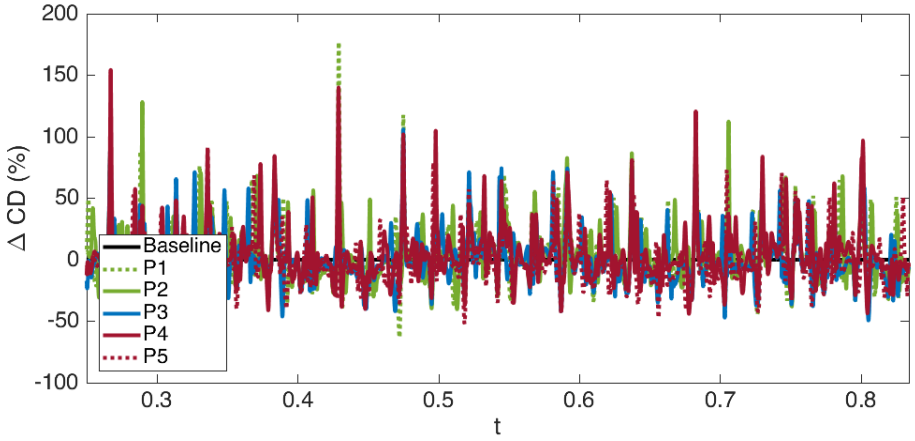

(a) ΔCD

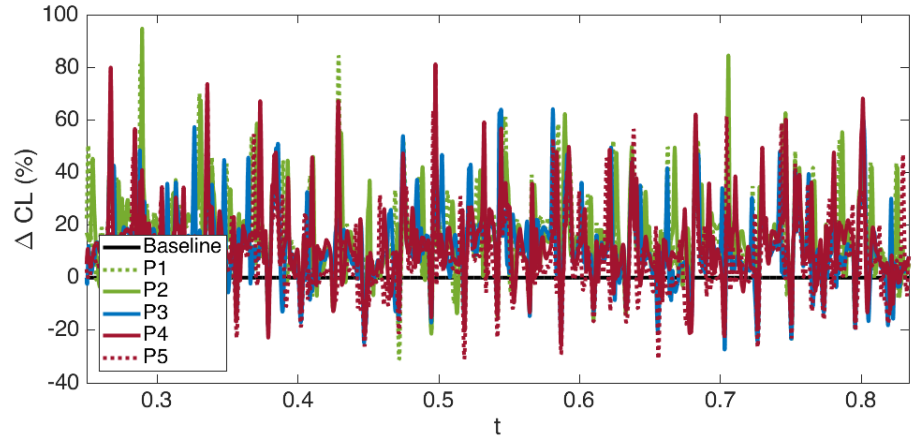

(b) ΔCL

Figure 15 – Instantaneous ΔCD and ΔCL with respect to the base line configuration on the wing of the NGCTR-TD for different positions of the ZNMF devices, case 3.

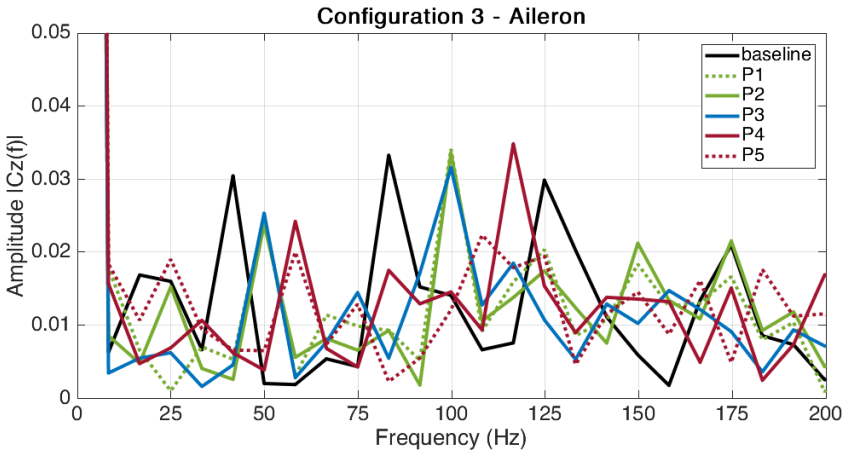

Figure 16 – FFT analysis of the CZ on the aileron for case 3.

7. Concluding remarks

Results of CFD simulations using Zero Net Mass Flux (ZNMF) devices for active flow control on the Next Generation Civil Tilt Rotor Technical Demonstrator (NGCTR-TD) aircraft were presented for 2 critical cases. It was found that these devices could reduce flow separations in critical flow regions, as for example the wing-fuselage and wing-nacelle junction. On the aileron the ZNMF devices permitted to increase the aerodynamic efficiency by 15%.
On-going studies focus on finding the optimal locations to place the ZNMF devices, and to verify the optimal operating parameters as the ZNMF jet actuation frequency and the jet velocity.

Acknowledgments

The results presented in this paper are obtained in the CleanSky2 project AFC4TR (funded by the European Union H2020 programme under Grant Agreement 886718). This work was granted access to the HPC resources of CINES/IDRIS/TGCC in France under the allocation made by GENCI and HPC Strasbourg. Leonardo Helicopters is acknowledged for providing the geometry, calculation conditions and their support in performing the simulations.

References

[1] Flight Path 2050 Europe's Vision for Aviation, Report of the High Level Group on Aviation Research, EUR 098 EN, 2011.

[2] Cattafesta, L.N. and Sheplak, M.,
Actuators for Active Flow Control,
Annual Review of Fluid Mechanics, Vol. 43, No. 1, 2011.

[3] Ingard, U. and Labate, S.
Acoustic circulation effects and the nonlinear impedance of orifices,
The Journal of the Acoustical Society of America, Vol 22., 1950.

[4] Vos J.B., Rizzi A.W., Corjon A., Chaput E., Soinne E.,
Recent Advances in Aerodynamics inside the NSMB (Navier-Stokes Multiblock) Consortium,
AIAA paper 1998-0225, 1998.

[5] Hoarau Y., Pena D., Vos J.B., Charbonnier D., Gehri A., Braza M., Deloze T., Laurendeau E.
Recent Developments of the Navier Stokes Multi Block (NSMB) CFD solver,
AIAA Paper 2016-2056.

[6] Spalart, P.R. and Allmaras, S.R.
A One-Equation Turbulence Model for Aerodynamic Flows,
AIAA Paper 92-0439, 1992.

[7] SHur, M.L, Spalart, P.R., Strelets, M.K. and Travin, A.K.
A hybrid RANS-LES approach with delayed-DES and wall-modelled LES capabilities,
International Journal of Heat and Fluid Flow, Vol. 29, 2008.

[8] Langtry, R.B. and Menter, F.R.,
Transition modeling for general CFD applications in aeronautics,
AIAA paper 2005-522, 2005.

[9] Menter, F.R.,
Zonal Two Equation k-w Turbulence Models For Aerodynamic Flows,
AIAA Paper 1993-2906, 1993.

[10] Jameson, A.
Time Dependent Calculations Using Multigrid, with Applications to Unsteady Flows Past Airfoils and Wings,
AIAA Paper 91-1596, June 1991

[11] Yoon, S., Jameson, A
A Multigrid LU-SSOR Scheme for Approximate Newton Iteration Applied to the Euler Equations,
NASA-CR-179524, 1986

[12] Eglinger, E., Ternoy, F., Dandois, J., Aigouy, G., Betsch, E., Jaussaud, G., Fournier, M., and Claeyssen, F.,
High-performance Synthetic Jet Actuator for Aerodynamic Flow Improvement Over Airplane Wings,
ACTUATOR 2018: 16th International Conference on New Actuators, Bremen, Germany, 25-27 June, 2018.

Copyright Statement